S1

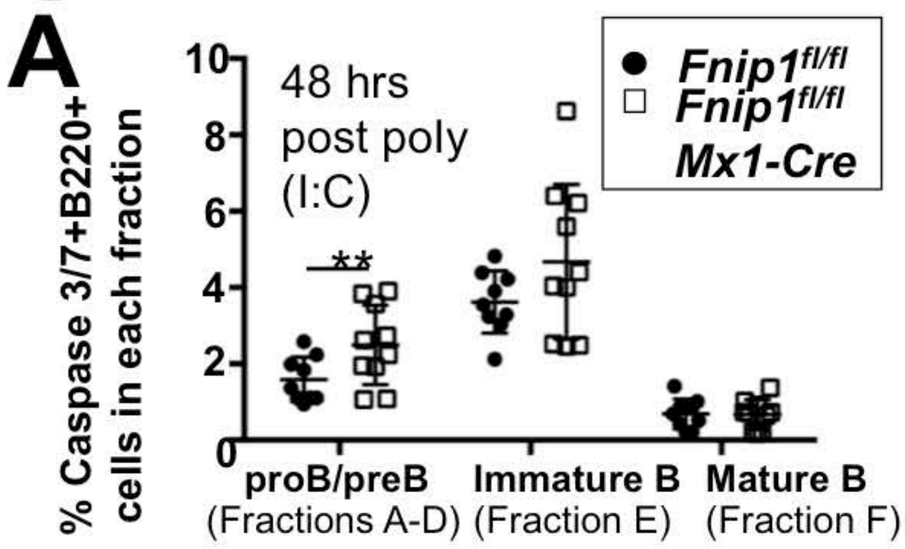

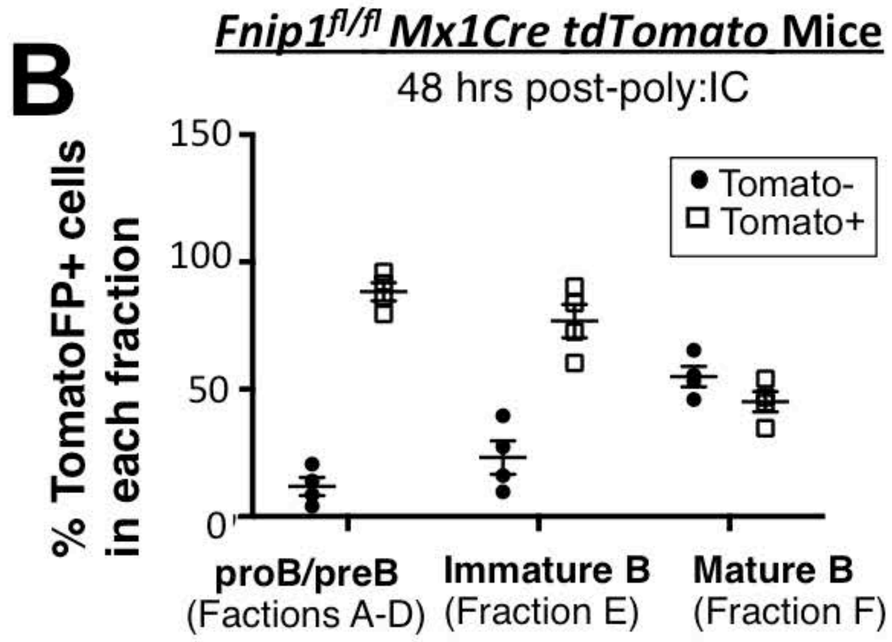

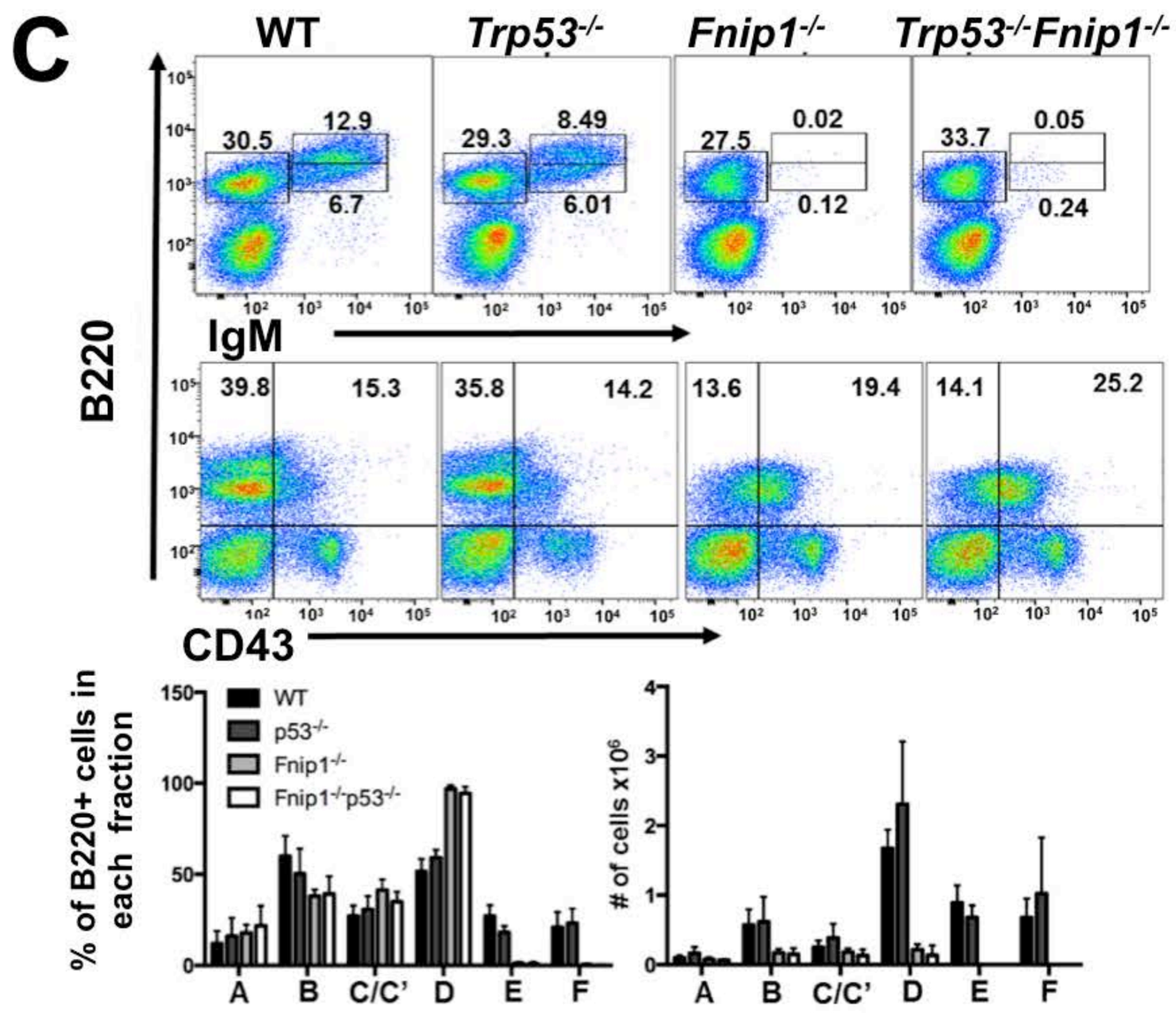

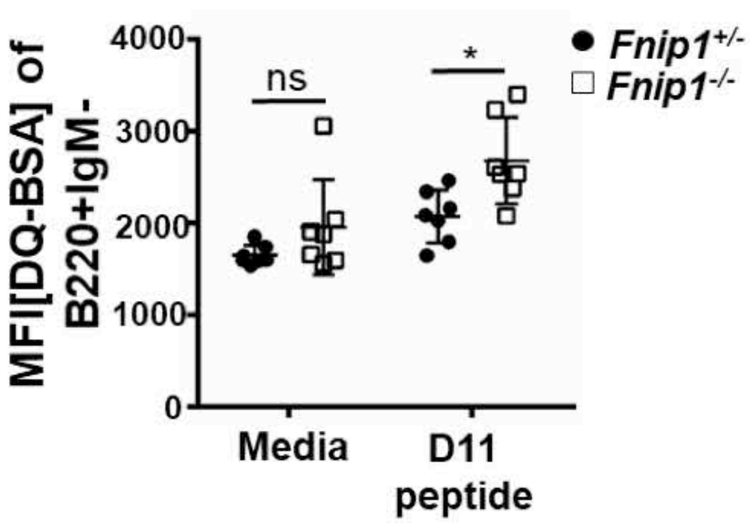

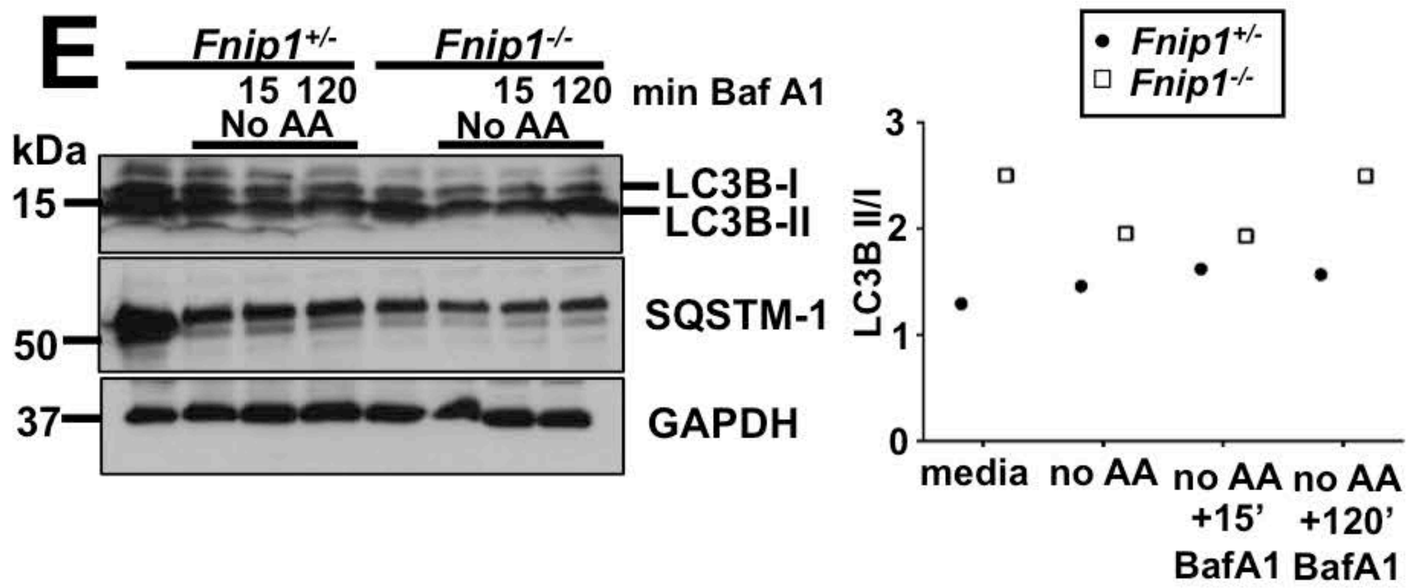

Figure S1. Disruption of *Fnip1* results in impaired B cell development and increased p53 independent apoptosis, and *Fnip1*-null pre-B cells exhibit increased autophagy. (A) Flow cytometric analyses of bone marrow (BM) cells from *Fnip1*$^{fl/fl}$ or *Fnip1*$^{fl/fl}$ *Mx1Cre* mice 48 hrs after deletion via poly I:C injection. Frequencies of cleaved Caspase 3/7 substrate in BM in pro-B/pre-B (B220^{+}IgM^{-}), immature B (B220^{lo}IgM^{+}), mature B (B220^{hi}IgM^{+}) cells are shown. **(B)** Flow cytometric analyses showing the percentage of pro-B/pre-B (B220^{+}IgM^{-}), immature B (B220^{lo}IgM^{+}), mature B (B220^{hi}IgM^{+}) cells from *Fnip1*$^{fl/fl}$ *Mx1Cre*tdTomato mice that are tomato fluorescent protein (FP)+ or FP- 48 hrs post-poly I:C injection. Lymphocytes were gated by FSC/SSC. **(C)** Representative flow cytometric analyses of bone marrow (BM) cells from wild type (WT), *Trp53*$^{-/-}$, *Fnip1*$^{-/-}$ and *Fnip1*$^{-/-}$*Trp53*$^{-/-}$ mice. (top) Shown are gated lymphocytes (FSC/SSC) following staining for B220 (CD45R), IgM and CD43 (Ly48). Numbers on the plots represent the frequencies of the gated populations. (bottom) Bar graphs show developmental (Hardy) fractions representing frequency (left panel) and absolute number (right panel) of cells from these mice. Gating for fractions: A=B220^{+}CD43^{+}CD24^{-}BP-1^{-}, B=B220^{+}CD43^{+}CD24^{+}BP-1^{-}, C/C'=B220^{+}CD43^{+}CD24^{+}BP-1^{+}, D=B220^{lo}CD43^{-}IgM^{-}, E=B220^{lo}CD43^{-}IgM^{+}, F=B220^{hi}CD43^{-}IgM^{+}. (**D**) Scatter plots show mean fluorescence intensity (MFI) of proteolyzed DQ-BSA in BM pro- and pre-B cells (B220^{+}IgM^{-}) from *Fnip*$^{+/-}$ or *Fnip1*$^{-/-}$ mice. Cells were incubated with Tat-D11 (Beclin 1) peptide to induce autophagy. (**E**) Representative immunoblot performed on whole cell extracts from mouse embryonic fibroblasts derived from *Fnip1*$^{+/-}$ or *Fnip1*$^{-/-}$ mice cultured ex vivo with or without amino acids as well as after stimulation with Bafilomycin A1 for the indicated times (left panel). Densitometric analysis of this immunoblot is shown with LC3BII/I ratios plotted (right panel).

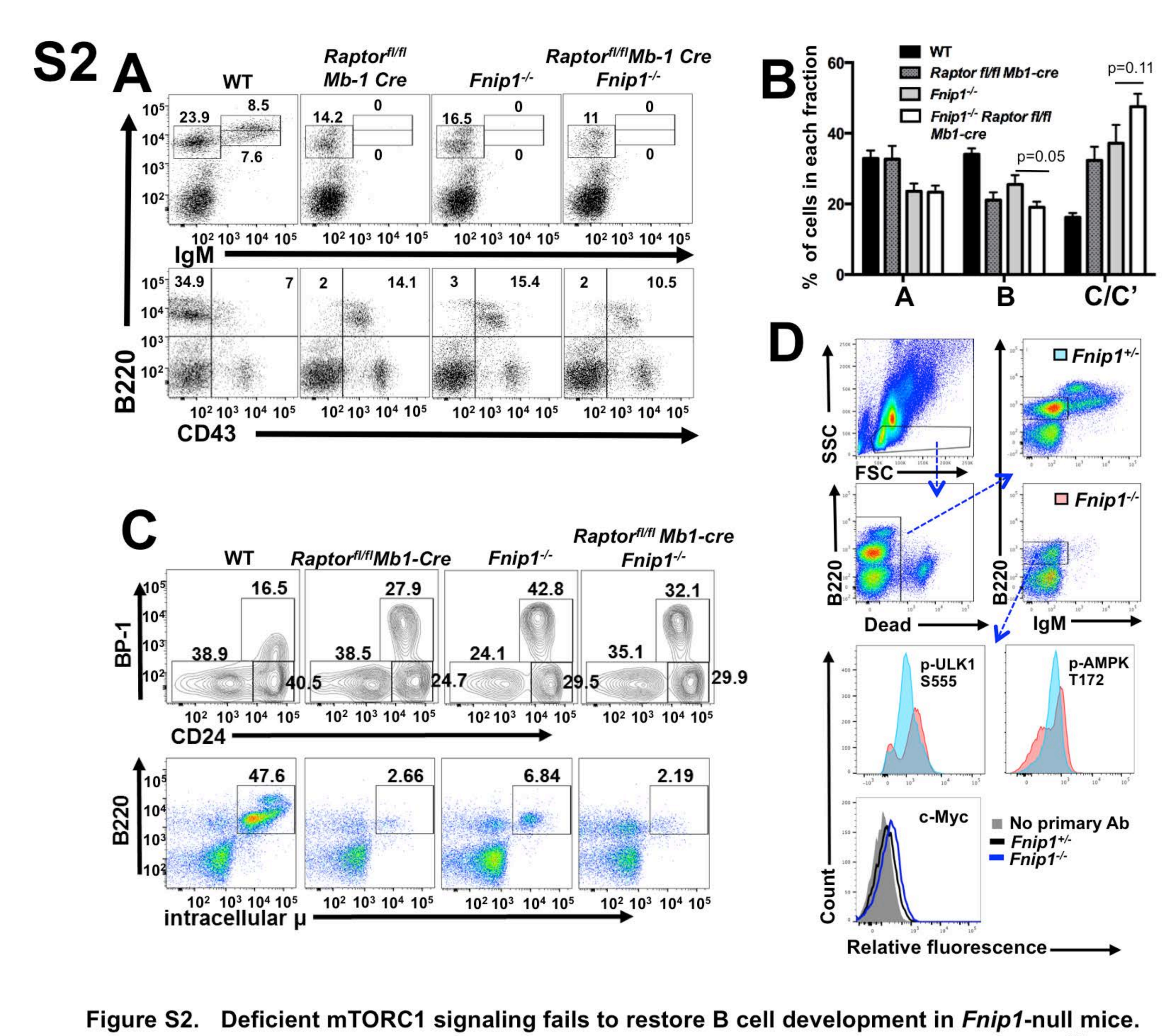

Figure S2. Deficient mTORC1 signaling fails to restore B cell development in *Fnip1*-null mice. (**A-C**) Representative flow cytometric analyses of bone marrow (BM) cells from WT, *Raptor$^{fl/fl}$Mb-1 Cre*, *Fnip1$^{-/-}$* or *Raptor$^{fl/fl}$Mb-1 Cre Fnip1$^{-/-}$* mice. (**A**) Dot plots show gated lymphocytes (FSC/SSC) following staining for B220, IgM and CD43. (**B**) Bar graph and **(C)** contour plots (top panel) are shown gated on lymphocytes and stained for B220, IgM, CD43, BP-1 (Ly-51, CD249) and CD24 (HSA) to show developmental (Hardy) fractions. Gating for fractions: A=B220^{+}CD43^{+}CD24^{-}BP-1^{-}, B=B220^{+}CD43^{+}CD24^{+}BP-1^{-}, C/C'=B220^{+}CD43^{+}CD24^{+}BP-1^{+}. (lower panel) Dot plots are shown gated on lymphocytes and stained for B220 and intracellular Igµ. **(D)** Gating strategy and representative examples of intracellular flow cytometric staining of *Fnip1$^{+/-}$* and *Fnip1$^{-/-}$* bone marrow cells (p-ULK1s555, p-AMPKT172, and c-Myc)

S3

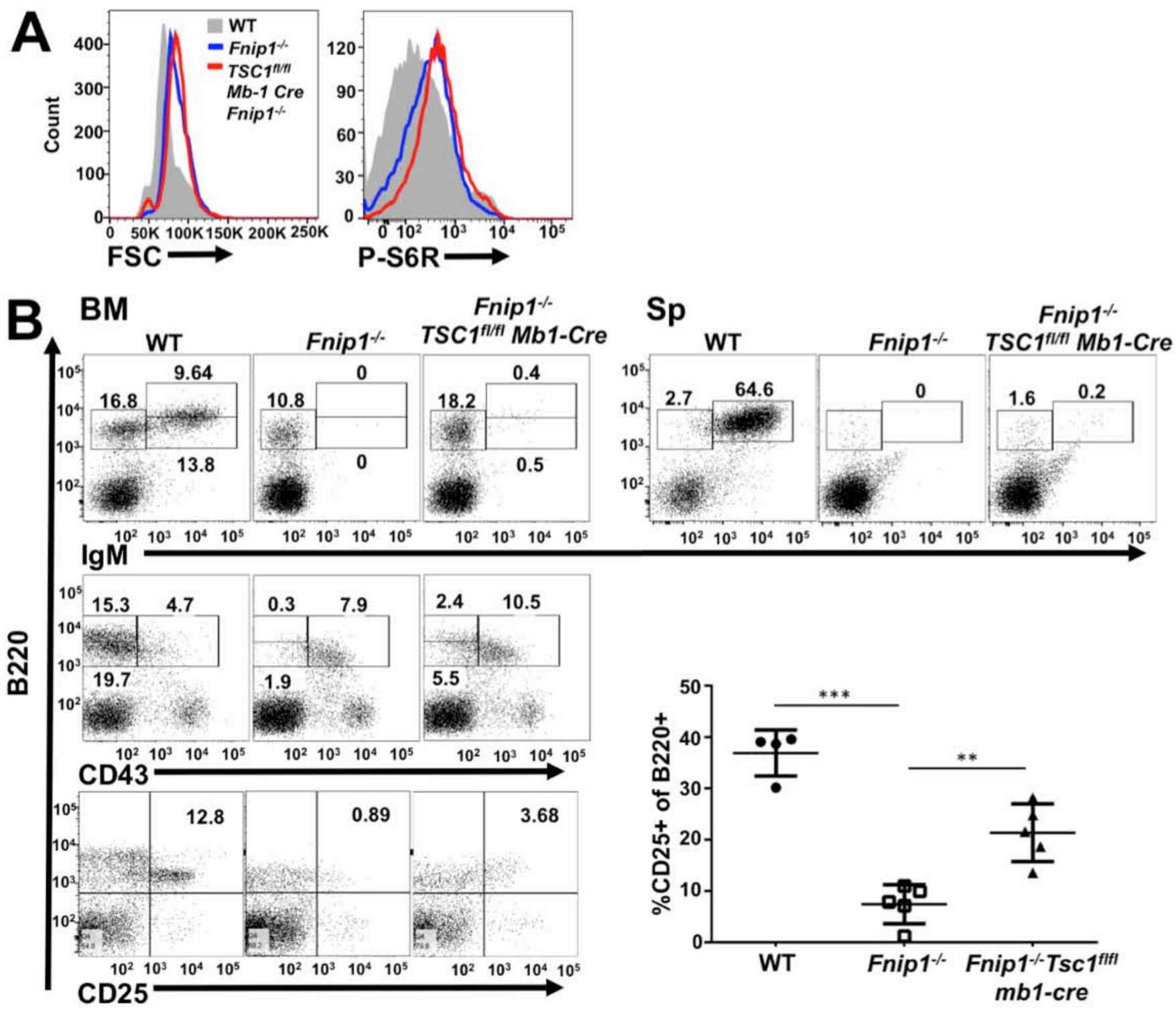

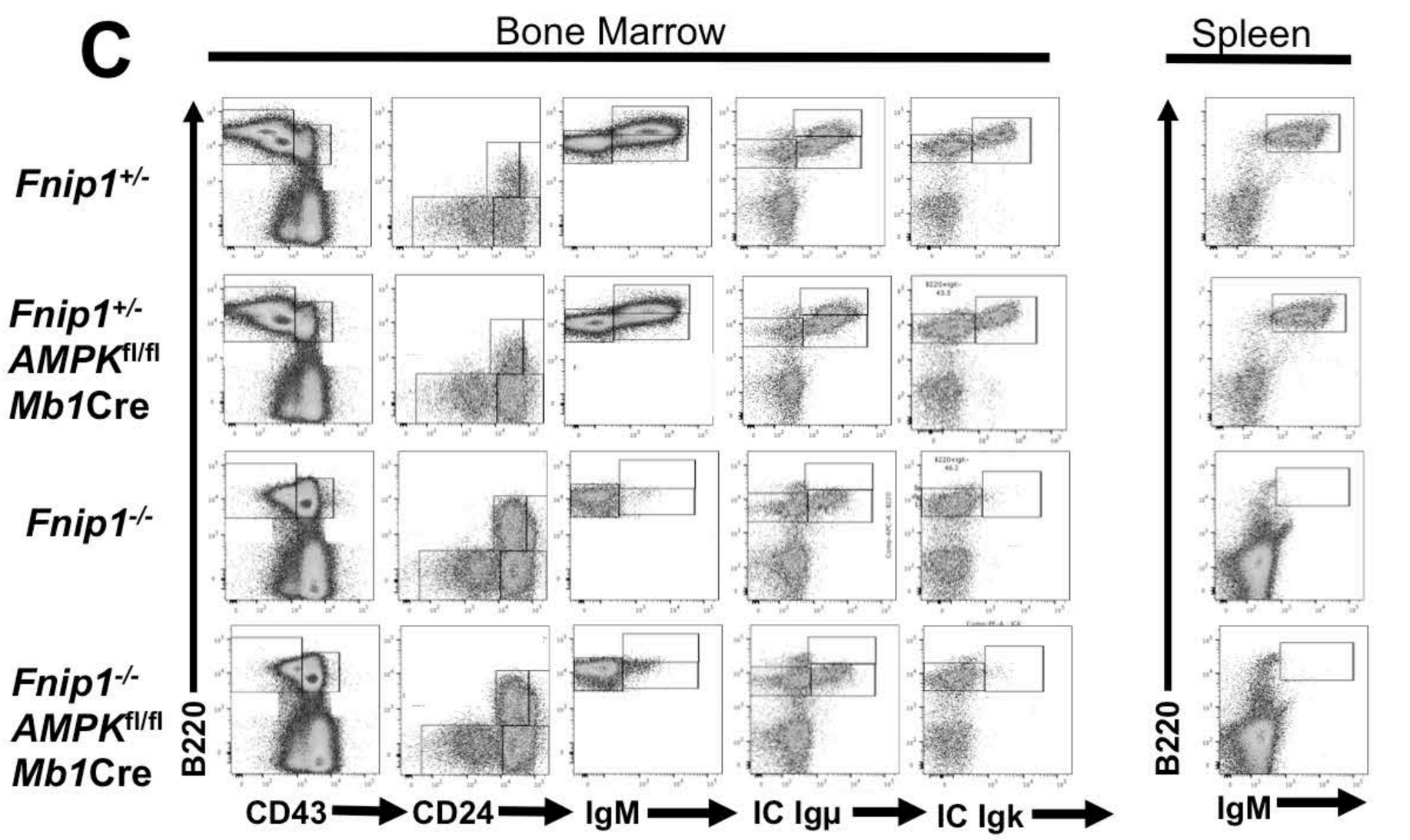

Figure S3. Increasing mTORC1-mediated cell growth or inhibiting AMPK fails to restore B cell development in *Fnip1*-deficient mice. (**A-B**) Representative flow cytometric analyses of bone marrow (BM) cells from WT, *Fnip1*$^{-/-}$ or *TSC1*$^{fl/fl}$*Mb-1 Cre Fnip1*$^{-/-}$ mice. Scatter plot (bottom right) shows frequency of CD25^{+} cells within the B220^{+} lymphocyte populations gated on FSC/SSC lymphocyte gate. (**C**) Representative flow cytometric analyses of bone marrow and spleen cells from WT, *Fnip*$^{+/-}$ *AMPK*$^{fl/fl}$*Mb-1 Cre, Fnip1*$^{-/-}$ or *Fnip1*$^{-/-}$ *AMPK*$^{fl/fl}$*Mb-1 Cre Fnip1*$^{-/-}$ mice.

Protein name	Relative abundance, *Fnip1* KO/HET
ADP-ribosylation factor 1	5.1
Leukocyte elastase inhibitor A	4.1
Transaldolase	3.1
Myosin light polypeptide 6	2.6
Small nuclear ribonucleoprotein-associated protein N	2.6
60S ribosomal protein L21	2.4
H-2 class I histocompatibility antigen, L-D alpha chain	2.1
T-complex protein 1 subunit epsilon	2
Splicing factor, proline- and glutamine-rich	2
Voltage-dependent anion-selective channel protein 1	2
Eukaryotic translation initiation factor 5A-1	1.9
60S ribosomal protein L6	1.7
Heat shock protein HSP 90-beta	1.6
40S ribosomal protein S11	1.6
Rho GDP-dissociation inhibitor 1	1.5
Glyceraldehyde-3-phosphate dehydrogenase	1.5
60S ribosomal protein L27a	1.5
60S ribosomal protein L12	1.5
Actin, cytoplasmic 1	1.3
40S ribosomal protein S3	1.3
Vimentin	0.4
Protein Mki67	0.3
Interferon regulatory factor 4	0.3
2',3'-cyclic-nucleotide 3'-phosphodiesterase	0.2
Methionine--tRNA ligase, cytoplasmic	0.2
Myosin light chain 4	0.05
Fc receptor-like A	0
Histone-binding protein RBBP7	0

Table S1. Mass spectroscopy of *Fnip1*-deficient pre- and pro-B cells reveals increased abundance of ribosomal proteins and actin consistent with mTORC1 activation.
Mass spectroscopy of Fnip1-deficient pre- and pro-B cells reveals increased abundance of ribosomal proteins and actin consistent with mTORC1 activation. Extracts were prepared from sorted pre- and pro-B ($B220^{+}IgM^{-}$) bone marrow cells from $Fnip1^{+/-}$ and $Fnip1^{-/-}$ mice. Identified proteins are listed which were relatively more abundant (yellow) or relatively less abundant (blue) in $Fnip1^{-/-}$ compared to $Fnip1^{+/-}$ cells. $P<0.05$ for all values shown using Students *t*-test.